RAPID COMMUNICATIONS

PHYSICAL REVIEW E VOLUME 47, NUMBER 1 JANUARY 1993

Scaling properties of the shadowing model for sputter deposition

Joachim Krug*
IBM Research Division, Thomas J. Watson Research Center, Yorktown Heights, New York 10598

Paul Meakin
Department of Physics, University of Oslo, Box 1048, Oslo 0316, Norway

(Received 7 October 1992)

We analyze a deterministic, one-dimensional solid-on-solid model for sputter deposition where the local growth rate is a function $V(\theta)$ of the exposure angle θ. For long times an algebraic height distribution $N(h)\sim h^{-(1+p)}$ develops, where the exponent p depends on the behavior of $V(\theta)$ close to $\theta=\pi$ and the extremal statistics of the substrate roughness. Analytic predictions for p, based on scaling arguments, are verified by large-scale simulations using a hierarchical algorithm.

PACS number(s): 05.40.+j, 68.55.Jk, 81.15.Cd

A new growth instability associated with geometric shadowing has recently been explored by several groups [1–4]. The instability is expected to be relevant in processes such as sputter deposition, where particles approach a growing surface along randomly oriented, linear trajectories. As a result of shadowing, valleys receive less flux than hills, and initial variations in the topography are amplified. The numerical solution of the one-dimensional continuum equations [2] indicates that the fully developed surface structure consists of domed columns separated by deep grooves. Due to computational limitations, the long-time coarsening dynamics of the columnar structure [5] has been studied only within a Huygens-principle approach [6], which neglects shadowing.

A solid-on-solid approximation of the full shadowing dynamics, the grass model [3], was introduced by Karunasiri, Bruinsma, and Rudnick [1] (KBR). In this model the surface is represented by a discrete set of needle-shaped columns of zero width and heights h_i, arranged on the sites of $i=1,\ldots,L$ of a one-dimensional lattice with periodic boundary conditions. For each site, the exposure angle $\theta_i, 0\le\theta_i\le\pi$, describes the range of directions in which straight lines can be drawn from the tip of the column without intersecting any of the other columns or the substrate (Fig. 1). The growth rate of a column is then given by [7]

$$\frac{dh_i}{dt}=V(\theta_i)\ , \tag{1}$$

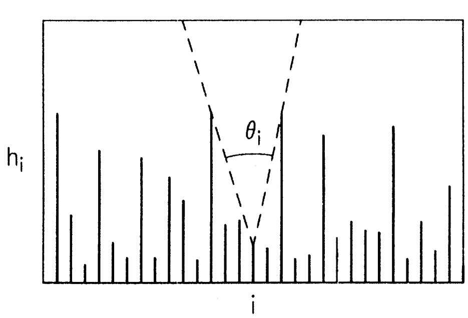

FIG. 1. A surface configuration generated with the grass model algorithm. The definition of the exposure angle is indicated.

where V is a monotonically increasing function of the angle with $V(0)=0$. KBR used $V(\theta)=R\theta$ with a rate constant R, corresponding to the assumption that the full flux arriving at the tip of a column contributes to its vertical growth. Other functional forms for $V(\theta)$ apply if the growth rate is taken to be proportional to the vertical *projection* of the particle flux [2], or if the particle source itself has a nontrivial angular distribution [8]. Starting from a random surface configuration, the shadowing instability was observed [1] to produce configurations with a "grassy" appearance (Fig. 1), characterized by an algebraic distribution of heights,

$$N(h)\sim h^{-(1+p)}\ , \tag{2}$$

where $N(h)dh$ is the expected number of columns with heights between h and $h+dh$. At time t, the power law (2) is cut off at the maximum height $h_{\max}=V(\pi)t$. The typical distance between columns that have not yet been affected by shadowing at time t, i.e., columns with $h_i(t)\approx h_{\max}(t)$, defines a *coarsening length scale* [4–6], which grows as

$$\xi(t)\sim t^p\ . \tag{3}$$

KBR found numerically that $p\approx1$, and gave a heuristic argument to explain this result.

The grass model provides an example of a physically relevant, nonlocal pattern-formation process, which is intermediate between the complexity of diffusion-limited growth [9,10] and the simplicity of unidirectional ballistic deposition [11], where the shadowing effect can be exactly reduced to a *local* interaction [12,13]. In the present paper we map out the universality classes of the grass model associated with the shape of the growth rate $V(\theta)$ and the statistics of the initial conditions. Throughout this work the initial values $h_i(0)$ are chosen independently at each site from a distribution $P_0(h)$ of finite support, $0\le h\le a$.

Our main results can be stated in terms of the behavior of $V(\theta)$ for small arguments, $V(\theta)\sim\theta^\eta$, the behavior close to $\theta=\pi$, $V(\pi)-V(\theta)\sim(\pi-\theta)^\alpha$, and the behavior of P_0 close to the maximum initial height a, $P_0(h)\sim(a-h)^\nu$. Here $\eta,\alpha>0$, and $\nu>-1$ to ensure the normalizability of P_0. The coarsening exponent p depends only on α and ν. For $\alpha \leq 1$ we find *strong universality* in the sense that $p=1$ independent of α and ν, while for $\alpha > 1$ p is given by

$$p = \frac{\nu+1}{\alpha(\nu+2)-1} . \tag{4}$$

The small-angle exponent η governs the long-time behavior of the typical (rather than average) column height. Depending on the value of η, shadowing may be either *complete* (almost all columns grow only to a finite height), or the typical height may diverge algebraically as t^{μ} with $\mu < 1$.

The starting point of our analysis is the dynamics of a single column at site 0, which is about to be shadowed by two columns at sites $\pm l$ with heights $h_l = h_{-l} = h_{\max} > h_0$. The exposure angle $\theta = 2\arctan[l/(h_{\max}-h_0)]$ is then easily seen to evolve according to

$$[1+\cot^2(\theta/2)]l\frac{d\theta}{dt} = -2[V(\pi)-V(\theta)] . \tag{5}$$

In the following we use (5) to model the shadowing dynamics in a situation where the coarsening length is l.

The first important observation is that (5) has two fixed points, at $\theta=0$ and π, and $d\theta/dt < 0$ elsewhere. The shadowing process can therefore be viewed as a transfer of the population of exposure angles from the unstable fixed point at π to the stable fixed point at 0. Not surprisingly, the two fixed points show up as distinct peaks in the distribution of exposure angles (Fig. 2). This implies that, although no column is ever completely shadowed in the sense that its growth rate would be strictly zero [14], it is possible to distinguish *active* and *shaded* columns according to whether the corresponding exposure angle is larger or smaller than some threshold angle θ_{th}. The shape of the distribution in Fig. 2 guarantees that the choice of $\theta_{\text{th}} \in (0,\pi)$ is arbitrary, since the vast majority of active (shaded) columns will reside very close to the unstable (stable) fixed point.

The scaling of the coarsening length ξ can be inferred from the behavior of (5) close to the unstable fixed point. The strategy will be to estimate the time $t^*(l)$ required for θ to move a finite distance (such that $\pi-\theta \sim 1$) away from the unstable fixed point, and then to identify $1/t^*$ with the *shadowing rate* (the rate at which active columns are lost). The density $n = 1/\xi$ of active columns decays as $dn/dt \sim -n/t^*$, so ξ grows according to

$$d\xi/dt \sim \xi/t^*(\xi) . \tag{6}$$

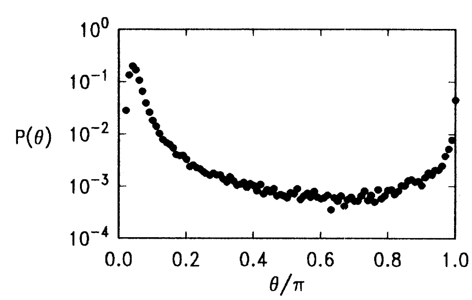

FIG. 2. Distribution of exposure angles for the grass model with $V(\theta)=\theta$, at time $t=20$. These data were obtained from 100 independent runs of a system of size $L=500$.

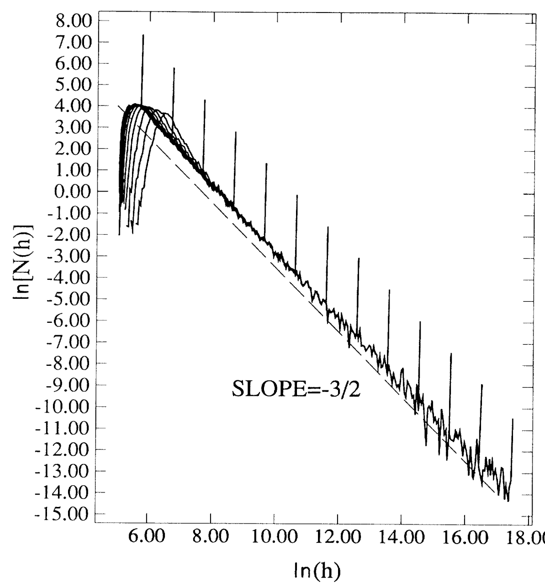

FIG. 3. Height distributions for the grass model with uniformly distributed initial conditions and growth rate $V(\theta)=\pi^{\alpha}-(\pi-\theta)^{\alpha}$ with $\alpha=\frac{3}{2}$, at times $t=2.65^n$.

Let $\theta(t)=\pi-\epsilon(t)$ with initial value $\epsilon(0) \ll 1$. Expanding (5) and using $V(\pi)-V(\theta) \sim (\pi-\theta)^{\alpha}$ we find $l\, d\epsilon/dt \sim \epsilon^{\alpha}$. For $\alpha < 1$ this yields $t^* \sim l$ independent of the initial value $\epsilon(0)$. Using (6) this implies that ξ grows linearly in time, i.e., $p=1$ as claimed above. In contrast, for $\alpha > 1$, t^* depends on the initial condition $t^* \sim l/[(\alpha-1)\epsilon(0)^{\alpha-1}]$. In order to apply this to the shadowing dynamics, we need to estimate $\epsilon(0)$ in terms of the coarsening length ξ. Clearly $\epsilon(0) \sim \delta h/\xi$, where δh is the typical height difference between two active columns. At this point it is crucial to realize that the columns that are active when the coarsening length is ξ had the *largest initial heights* in a region of size ξ; otherwise, they would have been shadowed already. For the bounded initial height distributions considered here, this implies that δh decreases with increasing ξ, since the eligible initial values are being squeezed towards the maximum initial height a. An elementary extremal statistics argument [13,15] shows that $\delta h \sim \xi^{-1/(\nu+1)}$ for initial height distributions that behave as $P_0(h) \sim (a-h)^{\nu}$ close to a. Thus $t^* \sim \xi^{\alpha+(\alpha-1)/(\nu+1)}$, and using (6) we obtain the formula (4) for the coarsening exponent. For a Gaussian or exponential initial distribution, δh depends logarithmically on ξ and we obtain $p=1/\alpha$, the $\nu \to \infty$ limit of (4). We also note that for $\alpha=2$, (4) coincides with the coarsening exponent for Huygens-principle growth [6]. Finally, in the borderline case $\alpha=1$ the dependence on the initial conditions is only logarithmic, $t^* \sim l\ln[1/\epsilon(0)]$, and we find $p=1$ up to logarithmic corrections, in agreement with KBR [1].

Next we turn to the discussion of our numerical results. We have developed a hierarchical algorithm that allows us to compute the exposure angles in a time of the order $L\ln L$. The growth rule (1) was discretized with a time increment chosen such that the height of the tallest column grows by 5% at each step in the simulation. The

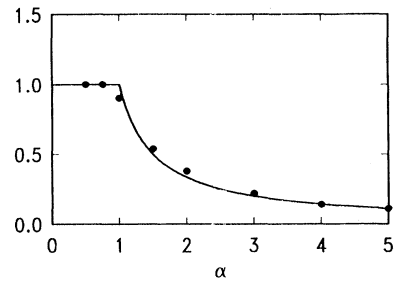

FIG. 4. Numerical estimates of the height-distribution exponent for the growth rate $V(\theta)=\pi^{\alpha}-(\pi-\theta)^{\alpha}$. The line is the prediction $p=\min\{[1,1/(2\alpha-1)]\}$.

accuracy was checked by simulations using maximum increments of 2.5% and 10%. Most of the data presented here were obtained by averaging over several runs with a system size of $L=32\,768$.

In Fig. 3 we show height distributions generated with the growth rate $V(\theta)=\pi^{\alpha}-(\pi-\theta)^{\alpha}$ with $\alpha=\frac{3}{2}$ and a uniform distribution of initial conditions ($\nu=0$) between 0 and $a=0.001$. The small amplitude of the initial roughness implies, by the arguments outlined above, a long inception time $t^*(1)\sim a^{-(\alpha-1)}$ before shadowing becomes effective. The data for earlier times have been omitted. Beyond a lower cutoff determined by the inception time we observe clean power-law scaling over five decades in h, with an exponent $1+p=\frac{3}{2}$ in agreement with (4). Note the peaks at $h\approx h_{\max}$ containing the population of active columns. Figure 4 summarizes the numerical estimates for p as a function of α. The agreement with (4) is seen to be excellent.

The dependence of the height distribution on the initial conditions is demonstrated in Fig. 5. We used the growth rate $V(\theta)=1-\cos\theta$, corresponding to $\alpha=\eta=2$, and the initial height distribution $P_0(h)=(1+\nu)(1-h)^{\nu}$, with $\nu=2$ and $-\frac{1}{2}$.

In Fig. 6 we explore the significance of the small-θ behavior of $V(\theta)$, using the family of growth rates $V(\theta)=(1-\cos\theta)^{\eta/2}$ and a uniform initial distribution ($\nu=0$). For small values of η ($\eta\leq 1$) a distinct peak appears in the height distribution in addition to the power-law tail with exponent $1+p=\frac{4}{3}$ (note that $\alpha=2$ independent of η). The peaks shifts to larger heights with increasing time, indicating that the background of shaded columns continues to grow. The peaks at different times

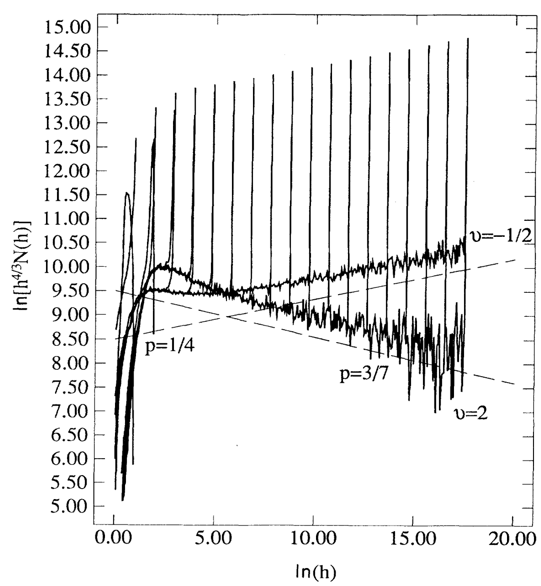

FIG. 5. Scaled height distributions $h^{4/3}N(h)$ for the grass model with $V(\theta)=1-\cos\theta$. The dashed lines indicate the prediction $N(h)\sim h^{-(1+p)}$ with $p=\frac{3}{7}$ for $\nu=2$, and $p=\frac{1}{4}$ for $\nu=-\frac{1}{2}$.

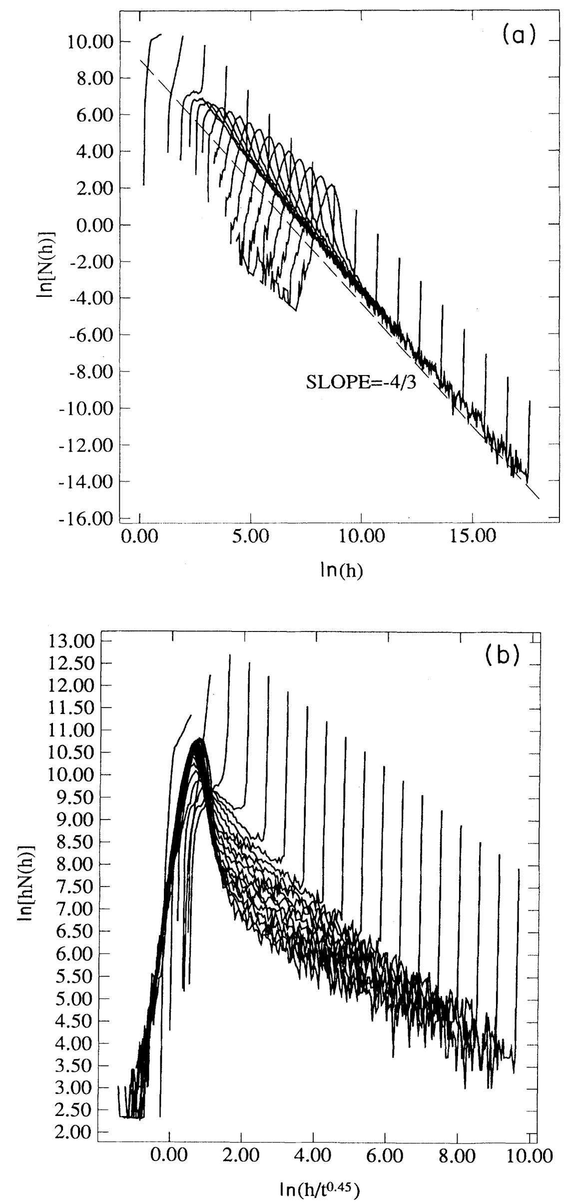

FIG. 6. Height distributions for the grass model with $V(\theta)=(1-\cos\theta)^{\eta/2}$, $\eta=0.75$, and uniform initial conditions. (a) shows the unscaled data and (b) demonstrates the approximate scaling form (7).

can be roughly superimposed using the scaling form

$$N(h,t)=h^{-1}f(h/t^{\mu}) , \tag{7}$$

where the prefactor h^{-1} is a consequence of the conservation of the total number of columns (the vast majority of columns belongs to the peak at late times). From plots of the kind shown in Fig. 6(b) we estimate $\mu \approx 0.825$ for $\eta = 0.25$ and $\mu \approx 0.45$ for $\eta = 0.75$. This behavior can be understood from an analysis of (5) for small θ. The angle is found to approach the stable fixed point as $\theta \sim l/t$, leading to the height of the shaded column increasing as

$$h \sim l^{\eta} t^{1-\eta} \tag{8}$$

for $\eta < 1$. As before, we now replace l by the coarsening length $\xi \sim t^p$ and find $\mu = 1-(1-p)\eta$, in reasonable agreement with the numerical estimates (here $p=\frac{1}{3}$).

However, this argument is consistent only if the further shadowing of shaded columns (with $\theta_i \ll 1$) continues to be dominated by the active columns (with $\theta_i \approx \pi$), rather than by other shaded columns. Otherwise, the relevant length scale in (8) would be smaller than ξ. The dominant shadowing from columns within a distance r of a shaded column is due to the largest column in that region, which, using the power-law distribution (2) [13,15], has a height of the order $r^{1/p}$. The corresponding shadowing angle $r^{1-1/p}$ *decreases* with r if $p < 1$. Hence for $p < 1$ the dominant shadowing indeed comes from columns at $r \approx \xi$ with heights $h_i \approx h_{\max}$. The argument breaks down for $p = 1$. Simulations using the growth rate $V(\theta)=\theta^{\eta}$, with $\alpha = p = 1$, indicate that in this case the relevant shadowing length scale l in (8) remains finite, leading to $\mu = 1-\eta$. Specifically, we estimate $\mu \approx 0.9$ for $\eta = 0.1$, $\mu \approx 0.6$ for $\eta = 0.5$, and $\mu \approx 0.3$ for $\eta = 1$, though the data collapse is less satisfactory than that shown in Fig. 6.

In summary, we have presented a detailed analysis of a deterministic solid-on-solid model for sputter deposition [1]. The subtle dependence of the scaling properties on the statistics of the random substrate is reminiscent of previous results for the Huygens-principle model of thin-film evolution [6] and certain deterministic models for unidirectional ballistic deposition [13]. However, the present model also exhibits a regime ($\alpha \leq 1$) where its properties are robust with respect to the initial conditions. Our approach has been to focus on the shadowing dynamics of a single column, which was then extended in a scale-invariant fashion. The method is similar in spirit to Rossi's treatment of the solid-on-solid approximation to diffusion-limited deposition [10]; however, due to the simpler nature of geometric shadowing, the analysis could be carried much further in the present case.

---

*Present address: IFF, Forschungszentrum Jülich, P.O. Box 1913, W-5170 Jülich, Germany.

[1] R. P. U. Karunasiri, R. Bruinsma, and J. Rudnick, Phys. Rev. Lett. **62**, 788 (1989); **63**, 693 (1989).

[2] G. S. Bales and A. Zangwill, Phys. Rev. Lett. **63**, 692 (1989); J. Vac. Sci. Technol. A **9**, 145 (1991).

[3] G. S. Bales, R. Bruinsma, E. A. Eklund, R. P. U. Karunasiri, J. Rudnick, and A. Zangwill, Science **249**, 264 (1990).

[4] C. Roland and H. Guo, Phys. Rev. Lett. **66**, 2104 (1991); J. H. Yao, C. Roland, and H. Guo, Phys. Rev. A **45**, 3903 (1992).

[5] R. A. Roy and R. Messier, in *Plasma Synthesis and Etching of Electronic Materials,* edited by R. P. H. Chang and B. Abeles (Materials Research Society, Pittsburgh, 1985).

[6] C. Tang, S. Alexander, and R. Bruinsma, Phys. Rev. Lett. **64**, 772 (1990); see also J. Krug and H. Spohn, Phys. Rev. A **38**, 4271 (1988) and *Solids Far from Equilibrium,* edited by C. Godrèche (Cambridge University Press, Cambridge, 1991), p. 533.

[7] We consider only the simplest case of pure shadowing, leaving the effects of surface relaxation and noise [1–4] to a future investigation.

[8] Strictly speaking, in these situations the growth rate depends separately on the right and left exposure angle $\theta_i^{R,L} = \min_{j>0}\{\arctan[j/(h_{i\pm j}-h_i)]\}$, rather than on their sum $\theta_i = \theta_i^R + \theta_i^L$. This complication is easily incorporated in our analysis.

[9] P. Meakin, Phys. Rev. B **30**, 4207 (1984).

[10] P. Meakin, Phys. Rev. A **33**, 1984 (1986); G. Rossi, *ibid.* **34**, 3543 (1986); **35**, 2246 (1987).

[11] P. Meakin, Phys. Rev. A **38**, 994 (1988).

[12] J. Krug and P. Meakin, Phys. Rev. A **40**, 2064 (1989).

[13] P. Meakin and J. Krug, Phys. Rev. A **46**, 4654 (1992).

[14] This is in contrast to unidirectional ballistic deposition [12,13], where columns are either completely shaded or completely independent of each other.

[15] E. J. Gumbel, *Statistics of Extremes* (Columbia University Press, New York, 1958).